Proceedings World Geothermal Congress 2020+1
Reykjavik, Iceland, April - October 2021

Resistivity Structure of Borinquen Geothermal Area, Costa Rica

Diego Badilla Elizondo, Gylfi Páll Hersir, Ásdís Benediktsdóttir

101 Reykjavik, Iceland

dabe@unugtp.is

Keywords: magnetotellurics, resistivity, high temperature, geothermal, Borinquen, Costa Rica

ABSTRACT

The resistivity structure of Borinquen Geothermal Area in Costa Rica was imaged by using 1D and 3D inversion of resistivity data. A total of 97 co-located MT/TDEM sounding pairs were used to carry out the inversion and to identify the main anomalies and structures controlling the area, in order to have a better understanding of the geothermal system and the geological setting. This is important for ICE (*Instituto Costarricense de Electricidad, Costa Rican Electricity Company*) due to the future develop of geothermal projects. The main geothermal signatures of a high temperature geothermal system were detected showing the different stages of alteration mineralogy. It is also suggested from the results the location of the north and northeast boundaries of the Cañas Dulces Caldera by analyzing resistivity and gravity data and comparing this information to well logs, geochemical data and inferred geological lineaments. Here it is proposed that Borinquen and Las Pailas Geothermal areas are mostly controlled by the north and northeast boundaries of the Cañas Dulces and San Vicente Caldera structures, connected through a main structure called here *Borinquen-Pailas*. Other geophysical/geological structures/fractures associated to this activity are also proposed in this work.

1. INTRODUCTION

In Costa Rica, exploratory studies of the geothermal potential started in the 70s in Guanacaste Volcanic Range (see Figure 1) located in the northwestern part of the country resulting in recommendations to investigate the areas on the slopes of Rincon de la Vieja, Miravalles and Tenorio volcanoes (Moya & Yock, 2007). Dr. Alfredo Mainieri Protti led geothermal research until 2013, which allowed the development of Miravalles GF (five power plants); Las Pailas GF (I and II), as well as the future Borinquen I and II geothermal power plants. Borinquen GF is located on the southwestern flank of Rincon de la Vieja Volcano whereas Las Pailas is to the south. Currently, Miravalles and Las Pailas fields are generating electricity for a total of ~253 MWe. Borinquen I will add ~55 MWe more by 2024 and Borinquen II ~55 MWe by 2030 resulting in a total of ~363 MWe.

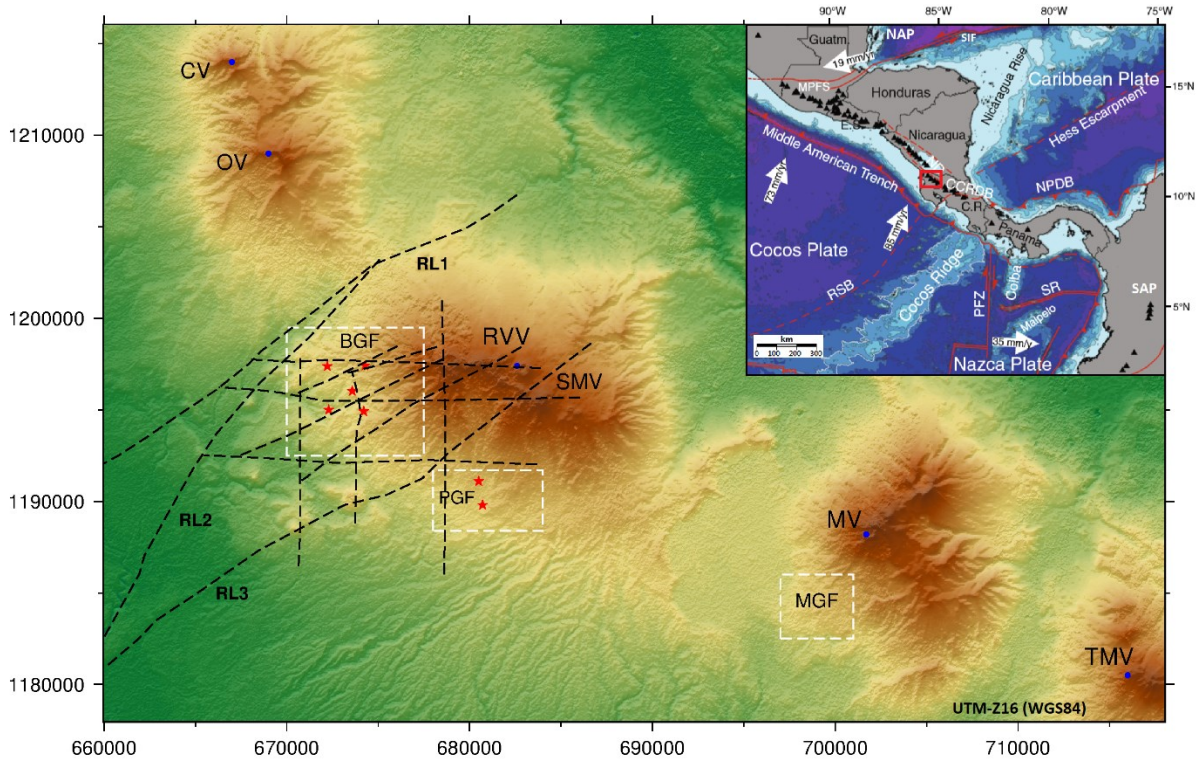

Figure 1: Map showing the location of Borinquen Geothermal Field (BGF), MGF, PGF (white dashed squares), Quaternary volcanoes (blue dots), geological lineaments (black dashed lines, adopted from Molina et al., 2014), deep wells (red star) and Santa Rosa Ignimbrite Plateau boundary (grey dashed line). Coordinates are in UTM-Z16 (m), generated from SRTM data. In the small map we show the tectonic setting of Central America (modified from Lücke, 2012) and the location of the study area (red square).

The overall objective of this work is to contribute to a better understanding of the geological setting of the Rincón de la Vieja Volcano Complex in the two geothermal areas located south and southwest from the edifice. The possible explanations of the geothermal system are key information for ICE to achieve the knowledge and experience necessary for the future developments, as it was visualized by Dr. Mainieri. It will bring to the country more possibilities to generate energy from renewables and continue aligned to the electric power generation and environmental expansion plans.

1.1 Electromagnetic methods in geothermal exploration

The application of electromagnetic (EM) methods to image the resistivity structure of geothermal prospects has been demonstrated to be successful. The use of MT and TDEM soundings during the exploration stage is widely reported (Árnason et al., 2010; Cumming and Mackie, 2010; Uchida, 2005). A resistivity model is key information to decide the location of exploration and possible production wells. This is because hydrothermal processes in geothermal systems affect the electrical resistivity of rocks; hence, models of the subsurface resistivity can be used to identify zones of different alteration, permeability and porosity (Rosenkjær and Oldenburg, 2012).

1.2 Resistivity structure of high temperature geothermal fields

The correlation between resistivity structure and hydrothermal alteration of rocks in geothermal systems is discussed in Árnason et al. (1986); Árnason et al. (2000); Hersir et al. (2009); Flóvenz et al. (2005) and Flóvenz et al. (2012). A low resistivity cap ($< 10\ \Omega$m) above a resistive core usually characterizes the resistivity structure of high temperature fields in volcanic rocks. There are a medium to high resistivity near surface layers representing unaltered cold rocks, below which a low resistivity cap delineates the smectite-zeolite zone which was formed at temperatures of 100 - 220 °C. In the temperature range of 230 - 240 °C the zeolites disappear and smectite is gradually replaced by the more resistive chlorite in the so- called transition zone or mixed- layer clay zone. Below this transition section, a more resistive epidote-chlorite zone if found, formed at temperatures exceeding 250 °C, also called the resistive core where the resistivity is dominated by surface conduction.

2. GEOLOGICAL SETTING

Central America (CA) is characterized by an internal magmatic arc developed in the oceanic crust of the Caribbean plate (see Figure 1, right up corner), below which the Cocos plate is subducted in a northeast direction at a convergence rate of 8.5 cm/yr (DeMets, 2001). It runs parallel to the Middle America trench (MAT) from the Mexico-Guatemalan border to central Costa Rica (CR). In the north-western part of Costa Rica it features as the Guanacaste Volcanic mountain range with an extension of ~75 km. Here, four Quaternary andesitic stratovolcanoes were formed (see Figure 1): Orosi (OV) – Cacao (CV), Rincon de la Vieja (RVV) - Santa María (SMV), Miravalles (MV) and Tenorio – Montezuma (TMV). The creation of this volcanic arc has consequently facilitated the formation of geothermal reservoirs. The formation of this geological structure was preceded by different periods of intense explosive silicic volcanism, generating several hundreds of cubic kilometres of ignimbrites and related deposits, which were emplaced in the period 6–0.65 Ma (Vogel et al., 2004). Kempter (1997) identified in the surroundings of the study area at least three caldera structures - Cañas Dulces, Guachipelín, and Guayabo – based on the spatial distribution of the deposits and by comparing the stratigraphy. This activity is associated with different caldera collapse events and it is probably responsible for these ignimbritic eruptions, their ages are 1.7 Ma, 1.5 Ma, and 1.4–0.6 Ma, respectively. Several authors discuss the origin and formation of the Cañas Dulces Caldera (CDC). More recently, Molina et al. (2014) combined information from deep boreholes drilled by ICE together with new geological work and radiometric dating to describe its stratigraphy, structure and volcanic evolution of the area.

The stratigraphy of the Borinquen Geothermal area can be summarized as: *Bagaces Group*, consisting of sequences of andesitic lavas, crystal tuffs and lithic tuffs, with a predominance of explosive products. *The Liberia Formation,* mainly constituted of massive pyroclastic flow deposits, dacitic to rhyolitic in composition, largely responsible for the formation of the Liberia ignimbrite. *The Canas Dulces Formation*, includes a group of seven dacitic domes containing phenocrysts of plagioclase, green hornblende, clinopyroxenes and orthopyroxenes, emplaced on the periphery of the southwestern border of the Cañas Dulces depression. *The Pital Formation*, includes dacitic pyroclastic sequences interbedded with minor epiclastic, lacustrine deposits and andesitic lavas. *Deposits of the Rincon de la Vieja volcano*, the uppermost stratigraphic unit and consists mainly of andesitic lava flows with subordinated pyroclastic deposits.

3. MT AND TDEM SURVEYS

The Borinquen geothermal area has been studied by ICE applying the MT method since the year ~2000 and TDEM sounding data have been collected since 2009. The total number of stations used in this work is 97 co-located MT/TDEM soundings as shown on Figure 2 (black dots).

The MT data were acquired using a typical field configuration for MT (Phoenix Geophysics, 2015). Five channels were recorded: two for the electric field (Ex, Ey) and three for the magnetic field (Hx, Hy, Hz) consisting of three coils that act as magnetic induction sensors. The magnetotelluric data were collected for frequencies ranging from 10400 Hz to 0.0001 Hz. The recording time for all the stations was always at least 20 hours. The separation between the different sites varied from 300 m and up to 700 m, with an average distance of about 500 m.

In the case of the TDEM sounding data, a typical central loop field configuration was used. A V8 receiver, T3 transmitter, RXU-TMR controller and respective transmitter and receiver loops were used. All of them manufactured by Phoenix Geophysics. A single turn 100 m by 100 m or two turns 50 m by 50 m side transmitter loop was used depending on the topography. Data were collected for two different frequencies (30 and 5 Hz). The acquisition time was on average 15 min.

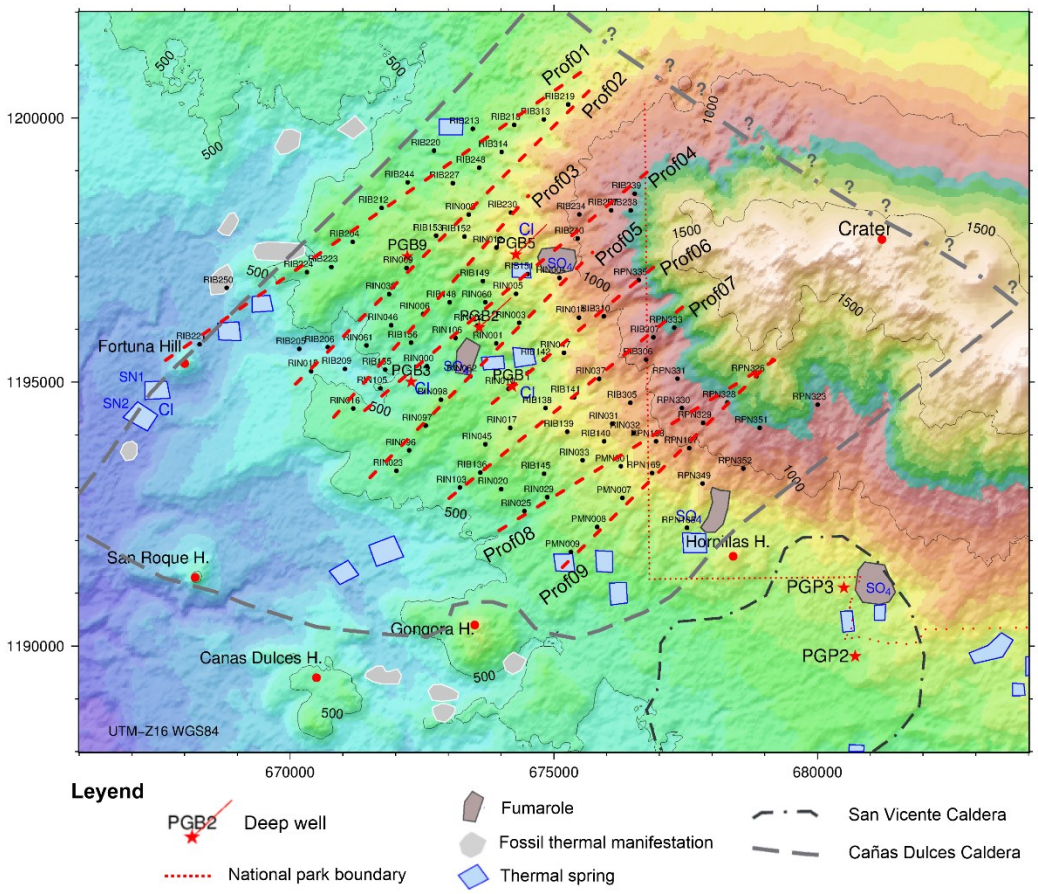

Figure 2: MT/TDEM stations in the prospect area (black dots), the location for the resistivity cross sections (red dashed lines), the deep wells (red star), the previously inferred caldera structures (grey dashed line- CDC, black dashed line- San Vicente Caldera), the hydrothermal manifestations and national park boundary (red dotted line)

4. DATA PROCESSING AND INVERSION

MT data were recorded as time series and thereafter they were Fourier transformed from the time domain to the frequency domain. In order to review or process data we require calibration files for the receiver and also for each coil sensor. Cross powers are created after running routines (robust processing or simple cross powers) that can substantially reduce the effect of noise present in the data files (Phoenix Geophysics, 2005). A solution for the relation between the electrical and magnetic field is found by solving the following equation:

$$\begin{bmatrix} E_x \\ E_y \end{bmatrix} = \begin{bmatrix} Z_{xx} & Z_{xy} \\ Z_{yx} & Z_{yy} \end{bmatrix} \begin{bmatrix} H_x \\ H_y \end{bmatrix} \tag{1}$$

where, $\boldsymbol{E}$ and $\boldsymbol{H}$ are the electrical and magnetic field vectors (in the frequency domain), respectively and $\boldsymbol{Z}$ is a complex impedance tensor which contains information about the subsurface resistivity structure.

From the impedances the apparent resistivity (ρ) and phases (θ) for each frequency are calculated according to:

$$\rho_{xy} = 0.2T\left|Z_{xy}\right|^2; \quad \theta_{xy} = arg(Z_{xy}) \tag{2}$$

$$\rho_{yx} = 0.2T\left|Z_{yx}\right|^2; \quad \theta_{yx} = \arg(Z_{yx}) \tag{2}$$

The calculated impedance tensor from the natural electric and magnetic field is finally exported into the industry-standard format EDI file (Wight, 1987) that contains the necessary information to use for geophysical interpretation/inversion software.

The processing of the TDEM sounding data consists in using a program that allows one to export the raw files into Universal Sounding Format (USF) file extension (Stoyer, 2010). A second quality control is done during this step. The USF file is read using Linux based program (TemX (Árnason, 2006a)) and exported into an *inv* file. Averages groups with the same frequency but different antenna effective area are used to calculate the apparent resistivity (Árnason, 2006a).

Once the files with the extension *inv* are created from the TDEM soundings a shell script program is created to link for each site both, the *inv* and the *EDI* files. Other parameters used by the software TEMTD (Árnason, 2006b) need to be set up to perform the 1D joint

inversion of the TDEM and MT data. Before that we also need to check if the EDI file contains all the information that we need, as for instance the rotational invariants from **Z**. In this work we used the determinant rotationally invariant for **Z**.

An electrical strike analysis was done by creating tipper strike and Zstrike maps. The static shift problem of the MT data was solved by the joint inversion with the TDEM data. Resistivity cross sections and depth-slices were created for the 1D case.

The data were prepared for the 3D inversion. A new joint inversion was performed for each mode, XY and YX, in order to correct the data prior to the 3D inversion. The data were resampled and plotted, a grid was designed and several routines were used to prepare the input data file. The code used for the 3D forward and inverse modelling is the WSINV3DMT code by Siripunvaraporn et al. (2005).

A sensitivity test was executed to evaluate the effects of the conductive seawater on the model response using different grids. Three initial homogenous half space models were assessed for resistivities of 10, 50 and 100 Ωm. A global relief model (ETOPO1) from Amante and Eakins (2009) was used to estimate the coastal lines and the depth to the sea floor to fix the cells in the sea to 0,3 Ωm.

The data set used for the 3D inversion were estimated as N = 97x30x4 = 11640 data points. After the sensitivity test, we decided that the dimensions of the problem are 54 x 54 x 35, in x, y and z directions respectively. The estimation for the numbers of unknowns was M = 102060 (more than 8 times the number of data points, respectively) which shows that it is an undetermined problem. Three different homogeneous half spaces were used as initial model for the 3D inversion: 10, 50 and 100 Ωm. The stitched 1D models were also used as initial model.

5. RESULTS AND DISCUSSION

In Figure 3 the geoelectrical strike based on the impedance for intermediate/great depth is presented. The main trends are suggested by white dashed lines after combining with the tipper strike. For great depth, the strike is aligned NW-SE. This preferential direction is associated to strike slip faulting systems, which are supposed to be mostly dextral motion (DeMets, 2001; Barahora et al., 2002; Climent et al., 2014; JICA, 2012) and that explains the existence of N-S structures (faults/fractures).

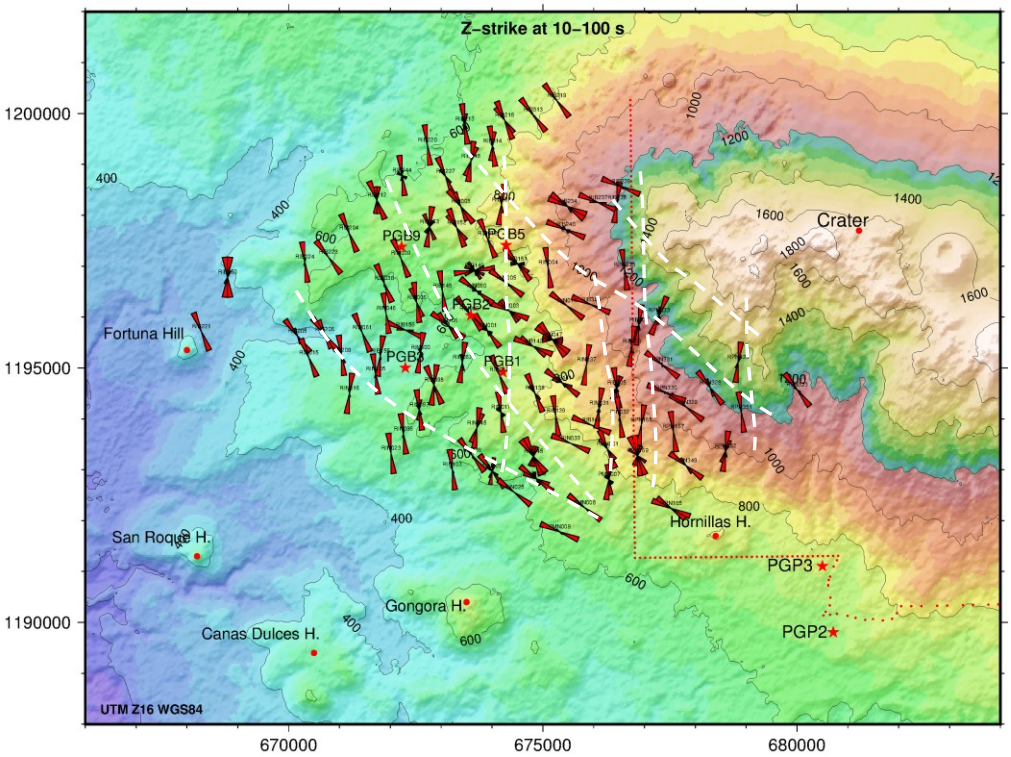

Figure 3: Impedance strike angle (Zstrike) for T=10 to 100 s. The white dashed lines represent the preferential directions combined with the tipper strike for the same period range

5.1 1D resistivity inversion results

In Figure 4 we present a resistivity cross section that runs close to three deep wells. The low resistivities reach the surface between soundings RIB151 and RIB240. This coincides with the hydrothermal manifestations (fumaroles) sampled east of PGB5 (see SO_4 label in Figure 2). A high resistive core appears underneath soundings RIN005 and RIB234 below 1 km depth (approximately at 250 m b.s.l). This resistive anomaly is explained by the presence of alteration minerals like illite, chlorite and epidote, suggesting

temperatures exceeding 250 °C as explained by Árnason et al. (1986). This is confirmed by the results of PGB5 (data from internal reports of ICE, geothermal department), where clearly illite/chloride are the dominant alteration minerals at those depths. It suggests what could be an upflow zone. To the southwest we can see how the resistivity doesn't reach values as high as to the northeast, which explains why in well PGB3 the temperature is not as high as expected.

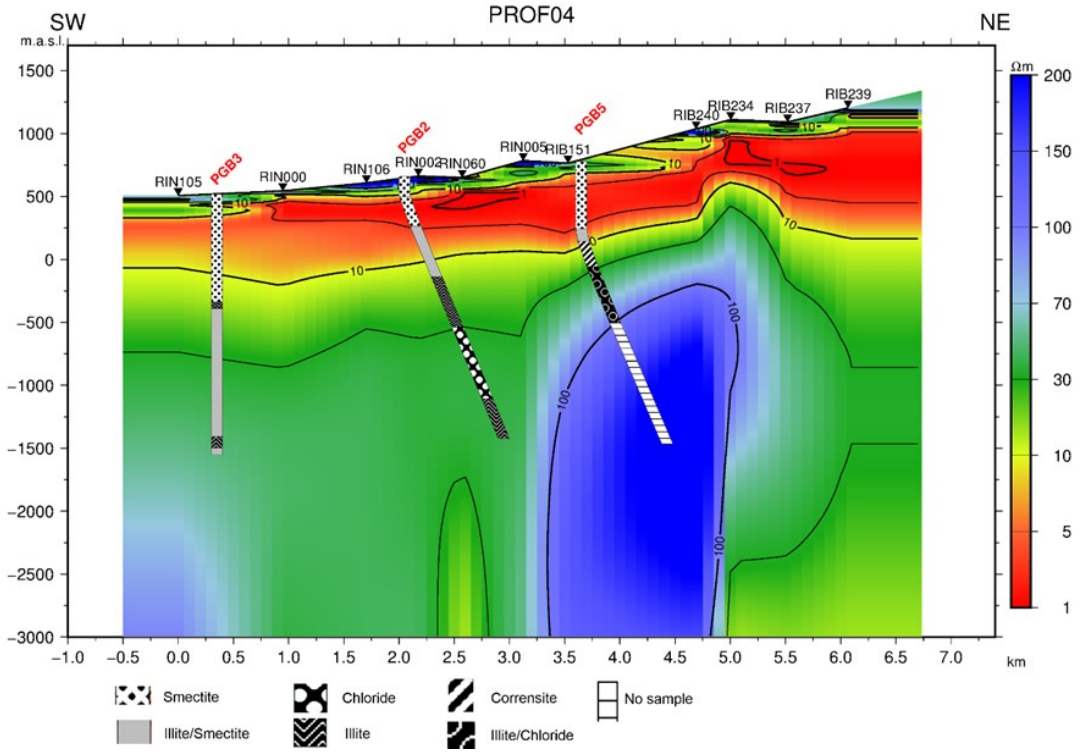

Figure 4: Resistivity cross section Prof04 showing the MT station number on top, deep well's name in red, and alteration mineralogy from well logs

The resistivity depth slices for the shallower part (<1 km depth) give a good indication of the distribution of the conductive layer and also suggest a NW-SE trend due to lateral discontinuities in NE-SW direction as it was seen for the resistivity depth slice at 500 m a.s.l. The transition from a conductive layer into a more resistive anomaly is seen in the central part of where resistivities higher than 10 Ωm are present. At 400 m b.s.l., ENE of PBG1, underneath and NE of PGB5 (~1400 m depth at those areas) high resistive anomalies appear which are directly associated to temperatures exceeding 250 °C. At 1000 m b.s.l. (see Figure 5) and below that elevation the resistivity starts to decrease at specific areas, for instance north of Las Hornillas Hill. Deep conductors appear ~3 km EES from PGB1 and PGB5, and NE of PGB5 at a depth of ~2000 m but these are more evident below ~3000 m depth. This anomaly of the resistivity structure is associated with the heat sources at depth.

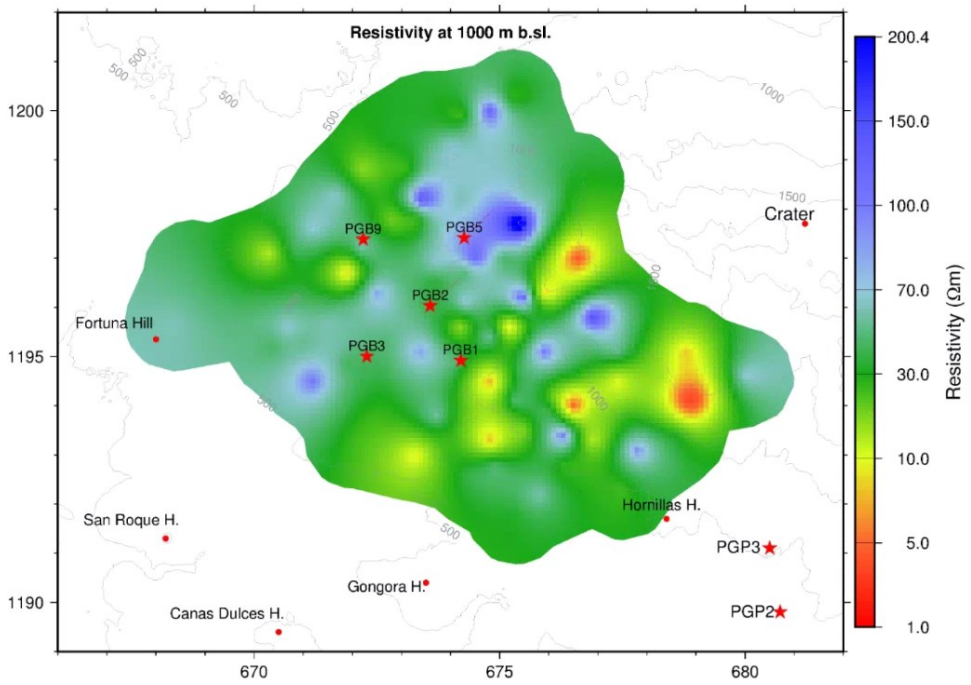

Figure 5: Resistivity depth slice at 1000 m b.s.l. based on the 1D inversion. Coordinates are in UTM-Z16 (km)

5.3 3D resistivity inversion results

The maps presented in Figure 6 and Figure 7 show the inversion results for the 10 Ωm homogeneous half space initial model. The fitting represented as RMS was in this case 1.25. At 350 m depth the conductive layer is distributed all over the area. It is mainly formed by smectite which has a high cation exchange capacity (CEC) (Lévy et al., 2018; Ingimarsson et al., 2016). In the depth slice on Figure 7 at 1300 m, the resistivity changes to higher values representing the occurrence of alteration minerals like illite and chlorite with lower CEC compared to smectite as it was found in the well logs and presented in Figure 4 for instance. In Figure 7 an important resistivity discontinuity is seen and represented by a blue dashed line which is consistent with the Zstrike and tipper strike. It could represent a boundary due to for example well PGB3 only reached 210 °C at the bottom whereas PGB1 went up to 277 °C. The conditions for wells PGB2 and PGB5 were also showing temperatures ~260 °C and located to the right of this structure. These results are fully presented in the Master thesis by Badilla (2019).

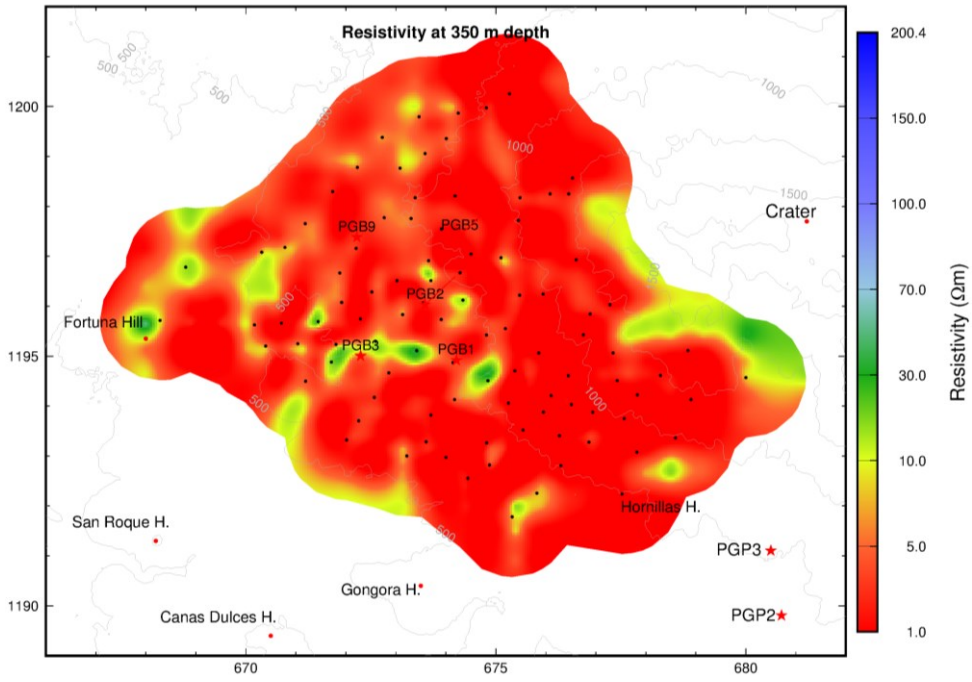

Figure 6: Resistivity depth slice at 350 m depth based on the 3D inversion. Coordinates are in UTM-Z16 (km)

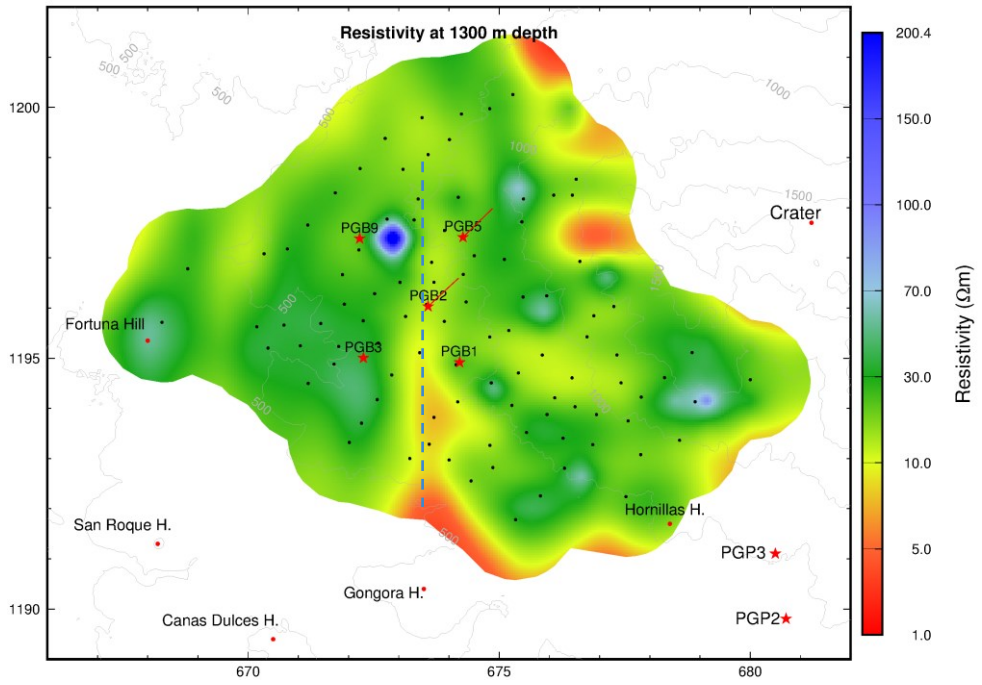

Figure 7: Resistivity depth slice at 1300 m depth based on the 3D inversion. Coordinates are in UTM-Z16 (km)

2. CONCLUSIONS

The main geothermal signatures associated to a high temperature geothermal system were mapped by using the 1D and 3D resistivity inversion approaches in Borinquen Geothermal area. The conductive layer presents a thickness varying between ~250 and ~800 m, and below it we find a mixed layer which most likely shows an increase in illite/chlorite. The resistivity increases especially to the north and northeast delineating the presence of a possible geothermal reservoir.

The low resistivities present at shallow depths in Borinquen GF forming what is considered the "clay" or "seal cap" are due to the high CEC of the minerals governing this layer, specifically smectite.

From the resistivity cross sections we can conclude that the geothermal reservoir is most likely located at least below 1 km depth.

The effects of the conductive sea water is mostly seen at low frequencies.

In the 3D inversion results, the model for the case of 10 Ωm as initial homogeneous model presented the minimum RMS after the forward calculation meaning that the most likely homogeneous half space resistivity of the area is ~10 Ωm.

The deep conductors associated to magmatic bodies (according to the 1D model) usually occur in the same depth range (~3 to 6 km) in Borinquen and Las Pailas (this work; Badilla; 2011; JICA, 2012) which probably represent the source for the formation of sills or dykes generating the hydrothermal alteration.

In this work the total delimitation of the Cañas Dulces Caldera is suggested. It was done by using the gravity results (Bouguer gravity map), the resistivity inversion models from the present work, the contributions from JICA (2012) and the results from Badilla (2011). We propose in this work the caldera boundaries to the north and northeast, and slightly different location of the boundaries to the southwest, south and southeast to the inferred in previous works.

REFERENCES

Amante, C. and B.W. Eakins. (2009). ETOPO1 1 Arc-Minute Global Relief Model: Procedures, Data Sources and Analysis. NOAA Technical Memorandum NESDIS NGDC-24. National Geophysical Data Center, NOAA. doi:10.7289/V5C8276M [07-03-2019].

Árnason, K., Haraldsson, G.I., Johnsen, G. V, Thorbergsson, G. Hersir, G.P., Saemundsson, Georgsson, L.S. and Snorrason, S.P. (1986). Nesjavellir: A geological and geophysical survey 1985. Orkustofnun report OS-86017/JHD02 96p. (in Icelandic).

Árnason, K. (2006a). TemX. A graphically interactive program for processing central-loop TEM data, a short manual. ÍSOR – Iceland GeoSurvey, Reykjavík, 10 pp.

Árnason, K. (2006b). TEMTD: A program for 1D inversion of central-loop TEM and MT data, a short manual. ÍSOR – Iceland GeoSurvey, Reykjavík, 16 pp.

Árnason, K., Eysteinsson, H., Hersir, G. P. (2010). Joint 1D inversion TEM and MT data and 3D inversion of MT data in the Hengill area, SW Iceland. Geothermics 39, 13-34.

Badilla, D. (2019). Resistivity structure of Borinquen Geothermal Area, Costa Rica: analysis of 1D and 3D inversion results. University of Iceland [master thesis].

Badilla, D. (2011). Resistivity imaging of the Santa Maria sector and the northern zone of Las Pailas geothermal area, Costa Rica, using joint 1D inversion of TDEM and MT data. UTP-GTP, Iceland, report 8, appendices, 49 pp.

Barahona, P., Bonilla, E., Cortés R., Guzmán, G., Herrera, P., Hidalgo, P., Martens, U., Méndez, J., Pérez, K., Reyes, K., Sjobohm, L., Vargas, C. & Zamora, N. (2001). Geología - vulcanología del campo geotérmico Borinquen – Las Pailas.- 162 págs. Universidad de Costa Rica [Bachelor thesis.].

Climent, A., Alvarado, G.E., Taylor, W. & Vargas, A. (2014). P.G. Las Pailas II Estudio de amenaza sísmica. - 42 págs. Instituto Costarricense de Electricidad (ICE), Costa Rica. [Internal report].

Cumming, W. and Mackie, R. (2010). Resistivity Imaging of Geothermal Resources Using 1D, 2D and 3D Inversion and TDEM Static Shift Correction Illustrated by Glass Mountain Case History. *Proceedings*, World Geothermal Congress, Bali, Indonesia, April 2010, 25-29.

DeMets, C. (2001). A new estimate for present-day Cocos Caribbean plate motion: Implications for slip along the Central American volcanic arc: *Geophys*. Res. Letters, 28, p. 4043–4046, doi:1 0. 1029 /2001GL013518.

Flóvenz, Ó.G., Spangenberg, E., Kulenkampff, J., Árnason, K., Karlsdóttir, R., and Huenges E. (2005). The role of electrical conduction in geothermal exploration. *Proceedings,* World Geothermal Congress 2005, Antalya, Turkey, CD, 9 pp.

Flóvenz, Ó.G., Hersir, G.P., Sæmundsson, K., Ármannsson, H., and Friðriksson, Þ. (2012). Geothermal Energy Exploration Techniques. In: Sayigh A, (ed.) Comprehensive Renewable Energy, Vol 7, pp. 51–9. Oxford: Elsevier.

Hersir, G.P., and Árnason, K. (2009). Resistivity of rocks. *Proceedings,* Short Course on Surface Exploration for Geothermal Resources. UNU-GTP and LaGe*o,* Santa Tecla, El Salvador, 8 pp.

Ingimarsson, H., Weisenberger, T.B., Hersir, G.P. & Flóvenz, Ó.G. (2016). Cation exchange capacity (CEC) analysis in well KJ-18 in Krafla and HE-42 and HE-46 on Hellisheiði, and the relation to electrical resistivity logs and alteration mineralogy. Vorráðstefna Jarðfræðafélag Íslands, April 8th, 2016, 17

JICA. (2012). Preparatory study for Guanacaste Geothermal Power Development Project in Costa Rica. Instituto Costarricense de Electricidad (ICE) [internal report].

Kempter, K. (1997). Geologic evolution of the Rincon de la Vieja volcano complex, northwestern Costa Rica. University of Texas, PhD thesis, 159 pp.

Lévy, L., Gibert, B., Sigmundsson, F., Flóvenz, Ó., Hersir, G., Briole, P. & Pezard, P. (2018). The role of smectites in the electrical conductivity of active hydrothermal systems: electrical properties of core samples from Krafla volcano, Iceland. *Geophysical Journal International*, Volume 215, Issue 3, December 2018, Pages 1558–1582, https://doi.org/10.1093/gji/ggy342

Lücke, O. (2012). Moho structure of Central America based on three-dimensional lithospheric density modelling of satellite-derived gravity data. International Journal of Earth Sciences: May 2012. doi 10.1007/s00531-012-0787-y

Molina, F., Martí, J., Aguirre, G., Vega, E. and Chavarría, L. (2014). Stratigraphy and structure of the Cañas - Dulces caldera (Costa Rica). Geol. Soc. Am. Bull., http:// dx.doi.org/10.1130/B31012.1 (published online 23 June 2014).

Moya, P. & Yock, A. (2007). Assessment and development of the geothermal energy resources of Costa Rica. UNU-GTP: Short Course on Geothermal Development in Central America – Resource Assessment and Environmental Management.

Phoenix Geophysics. (2005). Data processing. User's guide. Phoenix Geophysics, Ltd., Toronto, Canada.

Phoenix Geophysics. (2015). V5 System 2000 MTU/MTU-A User Guide. Version 3.0 July 2015, Toronto, Canada.

Rosenkjaer, G. and Oldenburg, D. (2012). 3D Inversion of MT data in geothermal exploration: a workflow and application to Hengill, Iceland. *Proceedings*, Thirty-Seventh Workshop on Geothermal Reservoir Engineering. Stanford University.

Stoyer, C. H. (2010). Universal Sounding Format. Interpex Limited Golden CO.

Uchida, T. (2005). Three-Dimensional magnetotelluric investigation in geothermal fields in Japan and Indonesia. *Proceedings*, World Geothermal Congress 2005 Antalya, Turkey, 24-29 April 2005.

Vogel, T., Patiño, L.C., Alvarado, G.E., and Gans, P.B. (2004). Silicic ignimbrites within the Costa Rican volcanic front: Evidence for the formation of continental crust: Earth and Planetary Science Letters, v. 226, p. 149–159.

Wight, D. (1987). MT/EMAP Data Interchange Standard. Society of exploration Geophysicists.